222 *Macromolecules* **2010**, *43*, 222–232
DOI: 10.1021/ma901966g

Macromolecules
ARTICLE

Homopolymers and Block Copolymers of *p*-Phenylenevinylene-2,5-diethylhexyloxy-*p*-phenylenevinylene and *m*-Phenylenevinylene-2,5-diethylhexyloxy-*p*-phenylenevinylene by Ring-Opening Metathesis Polymerization

Chin-Yang Yu, Masaki Horie, Andrew M. Spring, Kim Tremel, and Michael L. Turner*

Organic Materials Innovation Centre, School of Chemistry, The University of Manchester, Oxford Road, Manchester M13 9PL, U.K.

Received September 3, 2009; Revised Manuscript Received October 30, 2009

ABSTRACT: *p*-Phenylenevinylene-2,5-diethylhexyloxy-*p*-phenylenevinylene and *m*-phenylenevinylene-2,5-diethylhexyloxy-*p*-phenylenevinylene homopolymers (**3** and **4**) have been prepared by the ring-opening metathesis polymerization (ROMP) of strained cyclophanedienes, initiated by the second generation Grubbs catalyst. The as-formed polymers have a backbone of alternating *cis*- and *trans*-vinylene linkages due to the opening of only one vinylene of the cyclophanediene. Irradiation with UV light results in an isomerization to an *all-trans*-vinylene microstructure for all polymers. The polymer chain ends remain active after complete consumption of the cyclophanediene, and block copolymers can be prepared by addition of further cyclophanediene. The optical and electronic properties of the homopolymers and block copolymers are reported.

Introduction

Conjugated polymers have been widely studied for application in devices such as light emitting diodes,[1,2] field effect transistors,[3,4] and solar cells.[5,6] Polymers with a backbone of repeating phenylenevinylene units have attracted the most interest[7] and the majority of these reports concern homopolymers containing 1,4-substituted phenylene units, i.e., poly(*p*-phenylenevinylene) or PPV. Relatively few reports discuss the incorporation of 1,3-substituted phenylene units in the polymer backbone, i.e., poly(*m*-phenylenevinylene). A number of synthetic routes to phenylenevinylene polymers have been reported in the literature, e.g., pyrolysis of sulfonium polymer precursors (Wessling route),[8] dehydrohalogenation of xylylene dihalides (Gilch route),[9] polycondensation of xylyene diphosphonates with phthaldehydes (Wittig−Horner type condensation reaction),[10] and palladium-catalyzed polycondensation of divinylbenzene with dihaloarenes (Heck type condensation reaction).[11,12] A potential drawback of the reported routes is that there is little control over the polydispersity, molecular weight, or the end groups of the polymers. Moreover, it is well documented that small variations in the chemical structure of the polymer backbone can significantly influence the final optoelectronic properties.[13] Ring-opening metathesis polymerization (ROMP) offers the opportunity for precise control of polymer molecular weight, end groups, and low polydispersities. This method has been applied to the synthesis of polyacetylene by Feast[14] and Grubbs[15,16] and has been exploited in the synthesis of PPV polymers and copolymers by several groups. Initial reports focused on the preparation of precursors that could be converted to insoluble PPV homopolymer;[17−19] for example, ROMP of [2.2]paracyclophane-1,9-diene gives PPV as an insoluble, yellow fluorescent powder. Soluble copolymers of PPV have been prepared by ROMP of [2.2]paracyclophane-1,9-diene with cyclopentene, cyclooctene, and cyclocta-1,5-diene comonomers.[17−19] However, incorporation of more than 5% of PPV units gives insoluble polymers. Grubbs et al.[20] have demonstrated that PPV can be obtained by ROMP of functionalized bicyclo[2.2.2]octanedienes with excellent control of the polymer backbone structure. Final conversion to the conjugated PPV requires a high-temperature treatment (> 200 °C) and the presence of a base catalyst. PPV has also been prepared by ROMP of 9-[(*tert*-butyldimethylsilyl)oxy][2.2]paracyclophane-1-ene followed by thermal and chemical treatment.[13,21]

We recently demonstrated that soluble phenylenevinylene polymers can be prepared by the ROMP of alkoxy-substituted [2.2]paracyclophane-1,9-dienes in the presence of the second generation Grubbs catalyst.[22] This method gives polymers of controlled molecular weight, with a low polydispersity, very few chain defects, and an alternating *cis,trans*-microstructure. Controlled chain extension on addition of additional monomer showed that the chain ends remained active after complete monomer conversion. Recently, we communicated the application of this methodology to prepare phenylenevinylene block copolymers with 1,4- and 1,3-substituted phenylene units in the polymer backbone.[23]

Conjugated block copolymers are of considerable interest as these polymers can self-assemble into a variety of morphologies.[24−26] In conventional block copolymers the particular morphology adopted depends primarily on the volume fraction of the two blocks, the interaction between the blocks, and the molecular weight of each of the blocks.[27] A number of groups have examined the supramolecular assembly of A−B or A−B−A type rod−coil block copolymers containing one conjugated block. However, the commonly used coil blocks, such as polystyrene or poly(ethylene oxide), only support the self-assembly and do not carry any electronic function. This limits the optoelectronic response of this type of block copolymer in potential application, for example, in bulk heterojunction solar cells. Recently, fully conjugated rod−rod block copolymers have been reported, and these materials exhibit a different range of

*Corresponding author. E-mail: Michael.turner@manchester.ac.uk.

 Published on Web 11/25/2009 © 2009 American Chemical Society

Scheme 1. ROMP of DEHOPCPDE (1) and DEHOMPCPDE (2) (R = 2-Ethylhexyl) Using the Second Generation Grubbs Catalyst to Homopolymers 3 and 4

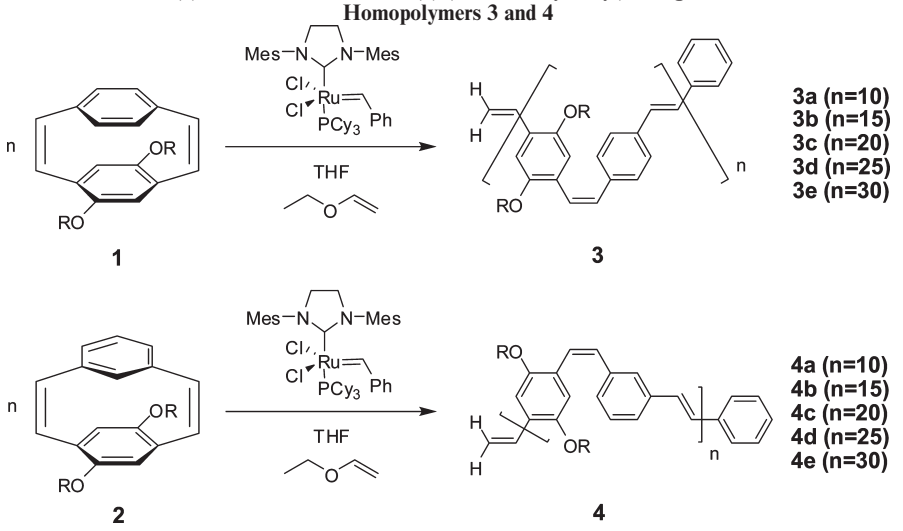

morphologies to those of the corresponding polymer blends or homopolymers.[26,28−34] In this paper we report the preparation of phenylenevinylene homopolymers and block copolymers with 1,4- and 1,3-substituted phenylene units via the ROMP of strained cyclophanedienes.

Results and Discussion

1,4-Phenylenevinylene and 1,3-Phenylenevinylene Homopolymers. ROMP of the diethylhexyloxy-substituted [2.2]paracyclophane-1,9-diene DEHOPCPDE (**1**) and the diethylhexyloxy-substituted [2.2]metaparacyclophane-1,9-diene DEHOMPCPDE (**2**) was initiated by addition of a THF solution of the second generation Grubbs catalyst (Scheme 1). The reaction mixture was heated at 40 °C, and the reactions were quenched by the addition of an excess of ethyl vinyl ether. The resulting polymers, **3** and **4**, were purified by filtering through silica gel and isolated by evaporation of the solvent. A range of polymer molecular weights were prepared by varying the initial monomer to initiator (Grubbs catalyst) ratio. Extended reaction times (20 h) were necessary to achieve complete conversion of monomer (as measured by TLC), indicating a slow rate of polymerization.[37,38]

The molecular weights of polymers **3** and **4** increased monotonically with initial monomer-to-catalyst ratio (Figure 1) with a correlation coefficient of 0.993 and 0.998, respectively. The polydispersities were in a range of 1.41−1.58 for polymer **3** and in a range of 1.30−1.46 for polymer **4**. The apparent discrepancy between the expected and the observed molecular weights is primarily due to the difference in the hydrodynamic radii of polymers **3** and **4** and the calibration standard employed for GPC, polystyrene.

The polydispersities of polymers **3** and **4** are higher than those seen in previous studies;[22,23] a possible explanation is that the rate of initiation is slow and that all of the active chain ends are not produced immediately at the start of the polymerization. The reactive nature of the polymer chains in this polymerization was confirmed by an experiment in which a second charge of monomer was added to a polymerization reaction (Figure 2). The initial reaction gave polymer **3** with a M_n of 7800 (expected M_n = 7004) and a polydispersity of 1.52. Chain extension with further addition of monomer increased M_n to 10 700 (expected M_n = 9304) with a similar polydispersity of 1.55. In the same experiment, ROMP of monomer **2** gave an initial polymer **4** with a M_n of

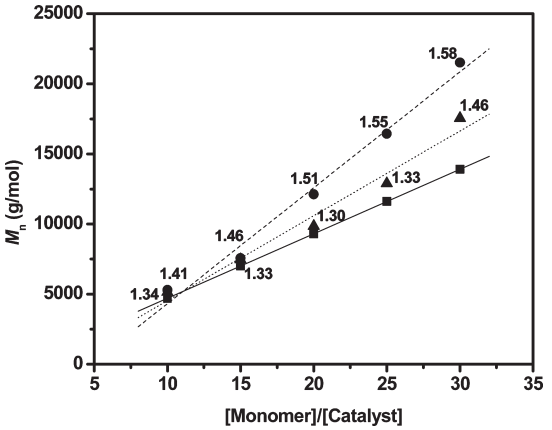

Figure 1. Dependence of molecular weight (M_n) of polymer on the monomer-to-catalyst ratio. The polydispersities are given for expected n = 10, 15, 20, 25, and 30. (●) Polymer **3**, (▲) polymer **4**, (■) calculated (including end groups).

7200 (expected M_n = 7004) and a polydispersity of 1.34. Addition of monomer **2** increased the M_n to 10 600 (expected M_n = 9004) with a similar polydispersity of 1.38. This is consistent with the polymer having active chain ends at complete monomer consumption and demonstrates the potential of this chemistry to prepare conjugated block copolymers.

The regiochemistry of the ring-opening reaction of monomers **1** and **2** was investigated by carrying out a reaction using a stoichiometric amount of the catalyst. Relief of significant ring strain within the monomers is achieved by opening of only one vinylene linkage, and it is expected that the products have one *cis*- and one *trans*-vinylene linkage with either the unsubstituted phenylene or the phenylene that carries the alkoxy groups bound to the ruthenium carbene. These experiments were essential to understand the microstructure of the polymer produced by ROMP of **1** and **2**. The stoichiometric reaction proceeded in THF at 40 °C and was monitored by TLC to confirm complete consumption of the monomer. The reaction mixture was then cooled to room temperature and quenched by addition of excess ethyl vinyl ether. The solvent was removed under reduced pressure, and the crude product was subsequently purified by filtering a DCM: hexane (1:1) solvent system through a short plug of silica. Two sets of peaks in a ratio of 1:0.8 for the vinyl end

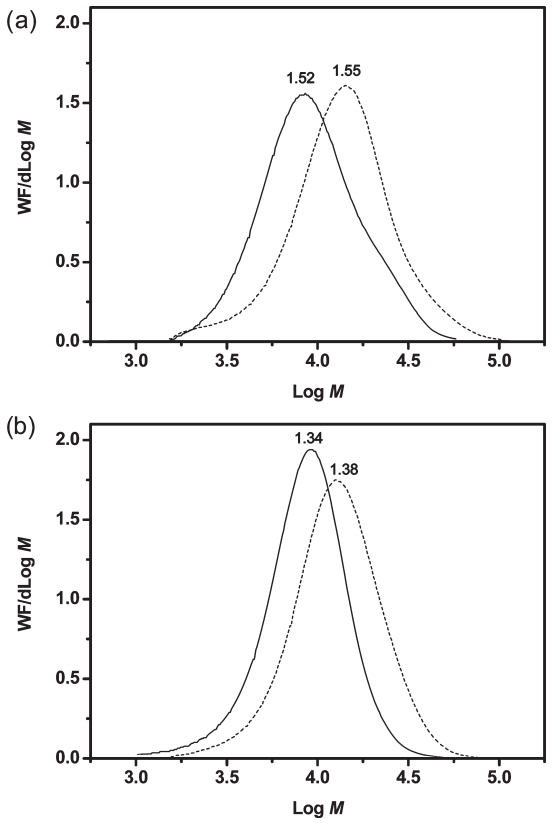

Figure 2. Molecular weight distribution for stepwise synthesis of (a) polymer **3** and (b) polymer **4** from $n = 10$ (solid line) to $n = 15$ (dashed line) using calculated Mark−Houwink parameters.

groups of ring-opening metathesis reaction of **1** were observed by ^{1}H NMR spectroscopy (Figure 3a). This indicates that the ring-opening reaction is not regioselective. Two major sets of peaks in a ratio of 1:0.4 were observed for the stoichiometric ring-opening of monomer **2** (Figure 3b). This indicates that there is a partial selectivity in the ring-opening reaction of **2**, but it is not complete.

The ^{1}H NMR spectra of polymers **3** and **4** indicated a *cis, trans* microstructure for the polymer backbone (see Supporting Information). Relief of significant ring strain within the monomers by opening a vinylene linkage leads to polymers with a backbone of regularly alternating *cis*- and *trans*-vinylene linkages. Peaks at 3.91, 3.48 ppm for **3** and peaks at 3.91, 3.41 ppm for **4** can be assigned to the hydrogens of the methylene groups attached to the oxygen for the *trans*- and *cis*-vinylene links of the polymer backbone, respectively.[39] Integration of these signals gave an approximately 1:1 ratio. Efforts to determine the ratio of alkene and aromatic hydrogens are difficult as the signals associated with these hydrogens overlap. However, the signals for *cis*-vinylene and *o*-phenyl hydrogens to the *cis*-vinylene groups were observed between 6.50 and 6.90 ppm. In addition, *trans*-vinylene and other aromatic hydrogens appear above 7.00 ppm. These assignments are in agreement with the model compounds prepared in the stoichiometric reaction. The molecular weights determined for polymers **3** and **4** are summarized in Table 1.

Absolute values for the degree of polymerization were determined by integration of the signals for the vinyl end groups observed at 5.24 and 5.76 ppm against those for the methylene groups attached to oxygen. These values are in general higher than that expected from the starting monomer:initiator ratio, indicating that the end group concentration is lower than expected. A plausible explanation for this discrepancy is a competing intramolecular backbiting reaction, and the products of this reaction pathway were identified in the MALDI-TOF mass spectra of polymers **3** and **4**. These show a major series of peaks (▲) separated by an interval of 460 mass units, corresponding to the molecular weight of the monomer (Figure 4); that is consistent with polymers that are terminated by vinyl and phenyl end groups (total mass 104), as expected. This series of peaks was accompanied by peaks associated with the addition of one sodium per polymer chain. A second main series of peaks (●) are observed at 102 mass units less than the major series. This series of peaks can be attributed to the formation of linear polymers with one less phenylenevinylene unit (C_8H_6, mass = 102) as intramolecular chain transfer to *cis*-vinylene linkages may occur before the capping reaction is carried out.[37] This observation is supported by the presence of a further series of peaks that are integral repeats of the monomer unit (460). These peaks can be assigned to low molar mass cyclic oligomers (■) that contain one more

Table 1. Molecular Weight Data for 3a−e and 4a−e (n = 10, 15, 20, 25, 30)

	M_n[a]	M_n[b]	M_w[b]	PDI[b]	M_n[c]
3a	4704	5300	7500	1.41	5700
3b	7004	7600	11100	1.46	8200
3c	9304	12100	18300	1.51	13300
3d	11604	16400	25500	1.55	18400
3e	13904	21500	33900	1.58	24700
4a	4704	5200	6600	1.33	5400
4b	7004	7500	9700	1.34	8100
4c	9304	9900	12800	1.30	10400
4d	11604	12900	17100	1.33	14000
4e	13904	17600	25700	1.46	19100

[a] Expected M_n (including end groups). [b] Determined by RI detector. [c] Determined by ^{1}H NMR.

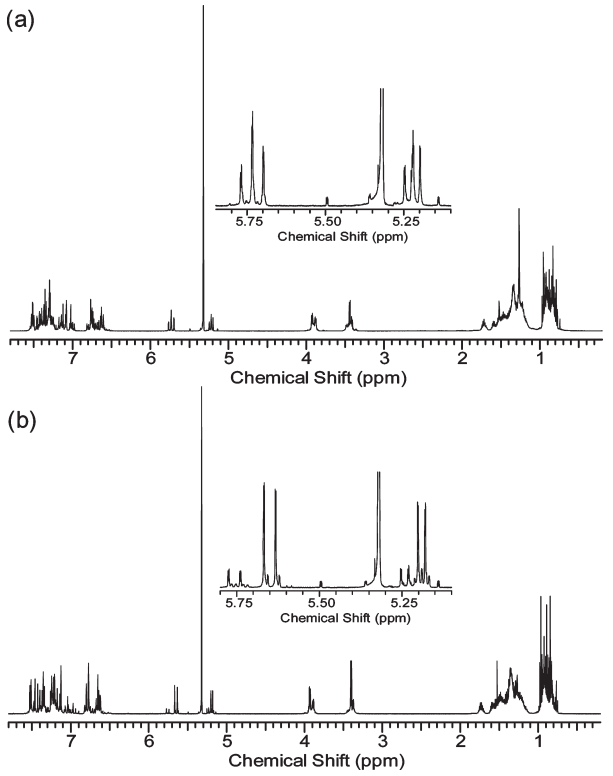

Figure 3. ^{1}H NMR spectra of stoichiometric study of ring-opening metathesis reaction of (a) monomer **1** and (b) monomer **2** in CD_2Cl_2.

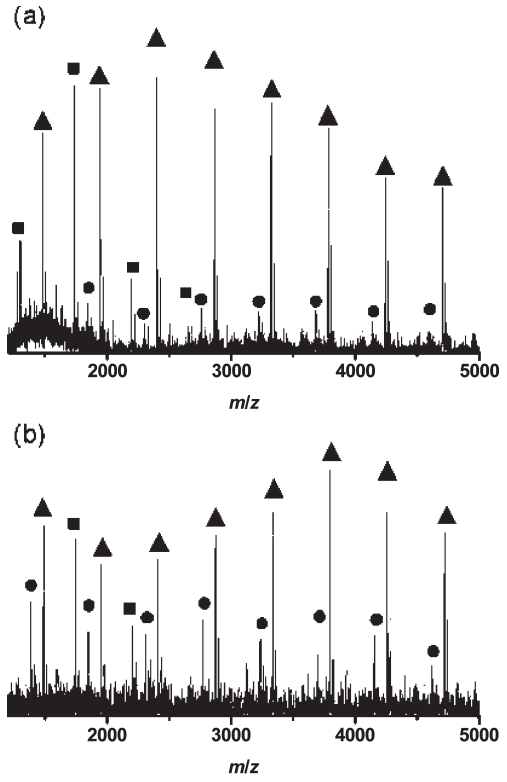

Figure 4. MALDI-TOF mass spectrum of (a) polymer **3a** and (b) polymer **4a** with an expected degree of polymerization of 10 repeat units.

diethylhexyloxy-substituted phenylenevinylene unit ($C_{24}H_{38}O_2$, mass = 358) and no end groups (loss of 104). There is no evidence for intermolecular chain transfer reactions as no peaks are detected for polymers with two phenyl or two vinyl end groups. The detection of only one series of linear polymers that are integral repeats of the monomer units (460) associated with intramolecular chain transfer suggests that chain transfer is restricted to the more active *cis*-vinylene units of the polymer backbone. Intramolecular chain transfer to the *trans*-vinylene linkages should lead a second series of peaks that are integral repeats of the monomer unit, containing even numbers of phenylenevinylene units; this series of peaks was not observed.

Isomerization of the *cis,trans*-microstructure to an *all-trans*-vinylene structure was expected to increase the conjugation length of the polymer and allow a direct comparison of polymers **3** and **4** generated by ROMP with phenylenevinylene polymers prepared by more conventional methods such as the Gilch route and the Wittig−Horner polycondensation. Polymers **3a**, **3c**, **3e** and **4a**, **4c**, **4e** can be isomerized to the *trans*-vinylene polymers **3f**−**h** and **4f**−**h** by prolonged irradiation at 365 nm in THF solution (10 mg in 10 mL). The reaction was followed by ^{1}H NMR spectroscopy (see Supporting Information) by measuring the ratio of the signal at 3.91 ppm to that at 3.48 ppm for polymer **3** and 3.91 ppm to that 3.41 ppm for polymer **4**, and complete conversion was achieved by irradiation for 36 h. The disappearance of the signals between 6.60 and 6.90 ppm associated with the *cis*-vinylene unit and the phenyl groups neighboring to *cis*-vinylene groups confirmed the isomerization to an *all-trans*-vinylene configuration.

The absorption and emission spectra of polymers **3a**−**e** and **4a**−**e** were recorded in dilute DCM solution (Figure 5). Polymer **3e** exhibited the longest conjugation length with an absorption maximum of 467 nm, which is red-shifted by 5 nm when compared to shortest conjugation length of **3a**. The fluorescence spectra recorded for **3a**−**e** show nearly identical emission spectra for all of the chain lengths with the emission peak at 527 nm and a shoulder at 566 nm. This is consistent with emission from the most conjugated region of chromophores in polymers **3a**−**e**, regardless of the chain length. The absorption maximum of the longest chain **3e** was slightly red-shifted by about 10 nm over that of an analogous polymer, poly(*p*-phenylenevinylene-*alt*-2,5-dioctyloxy-*p*-phenylenevinylene)s reported previously.[41] In addition, the emission maximum at 527 nm was also red-shifted by 10 nm when compared to that of polymers reported by Ferraris et al.[41] This was unexpected given the *cis,trans* microstructure of **3a**−**e** as the previously reported poly(*p*-phenylenevinylene-*alt*-2,5-dioctyloxy-*p*-phenylenevinylene)s were synthesized by Wittig−Horner polycondensation and had an entirely *trans*-vinylene microstructure. Polymers with *trans*-vinylene linkages are known to be more conjugated than the corresponding *cis*-vinylene polymers.[42] The more extended conjugation of polymers **3a**−**e** is due to the random ROMP of **1** that results in polymers in which the microstructure contains segments with two dialkoxyphenylene rings bound to a *trans*-vinylene unit. Emission from these segments is therefore expected to be red-shifted over the regularly alternating polymers prepared by Wittig−Horner polycondensation.[41]

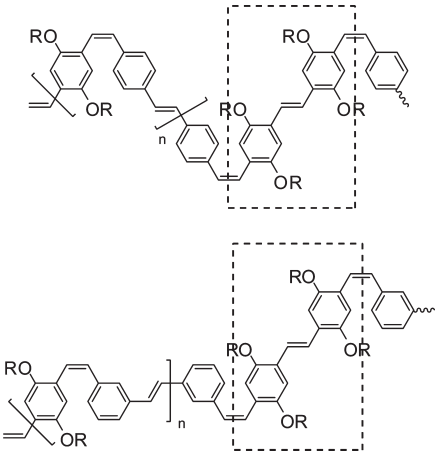

UV−vis spectra recorded for polymers **4a**−**e** exhibited two absorption bands. The longest polymer **4e** absorbed at 315 and 398 nm which were red-shifted by 2 and 3 nm when compared to the shortest length of polymer **4a**. The wavelength range of the maximum absorption and the small difference (3 nm) between **4e** and **4a** indicates that the *m*-phenylene linkages effectively interrupt the conjugation when compared to commercial MEH-PPV (λ_{max} = 480−500 nm) and **3a**−**e** (λ_{max} = 460−470 nm). The absorption spectra of **4a**−**e** were in agreement with previous reports for *m,p*-phenylenevinylene polymers.[43,44] The fluorescence spectra recorded for **4a**−**e** shows nearly identical emission spectra for all chain lengths with the emission maximum peak at 495 and a shoulder at 525 nm. Again, emission occurs from the most conjugated segment of the polymer, regardless of the chain length. Weak emission bands at around 450 nm were observed for the shortest chain length of the polymer, perhaps suggesting that energy transfer from the chain end segments was not complete. The emission maximum recorded for **4a**−**e** at 495 nm is red-shifted by 45 nm from values reported in the literature for comparable polymers prepared by Wittig−Horner polycondensation.[39,43,44] Again, the random nature of the ROMP of **2** gives polymer

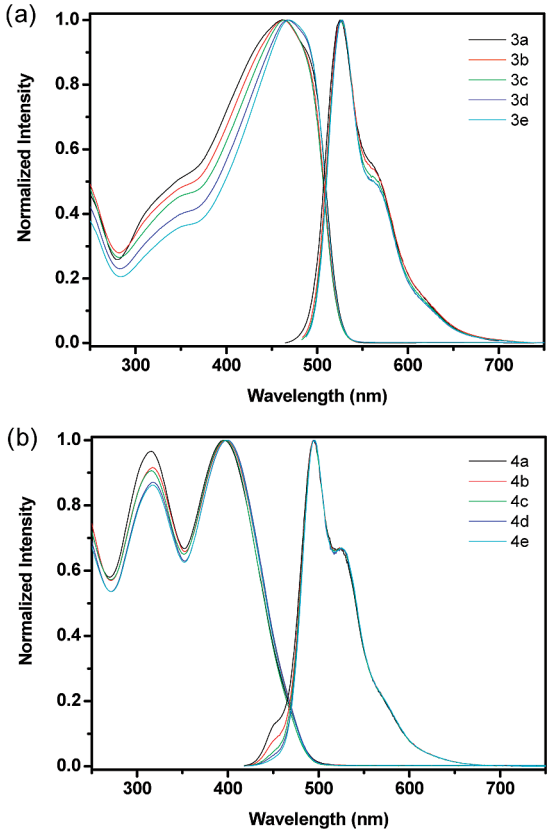

Figure 5. Solution UV−vis and PL spectra of (a) polymers **3a**−**e** and (b) polymers **4a**−**e**.

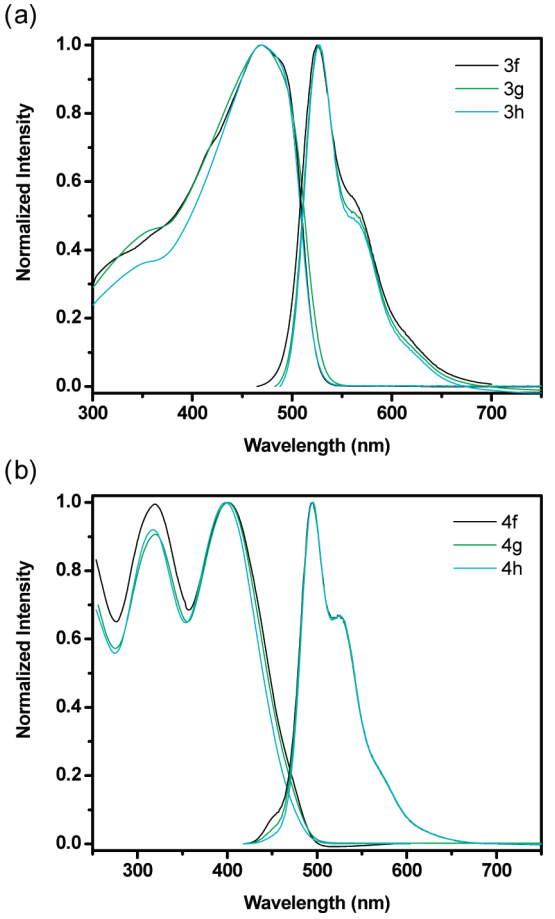

Figure 6. Solution UV−vis and PL spectra of (a) polymers **3f**−**h** and (b) polymers **4f**−**h**.

4 in which the polymer backbone contains segments with two dialkoxy-substituted *p*-phenylene rings bound to a *trans*-vinylene unit. Emission from these segments is therefore expected to be red-shifted from those prepared by simple polycondensation methods.

The solid-state absorption spectrum of **3e** shows a maximum absorption at 479 nm which is red-shifted by 9 nm from the solution value. The solid-state fluorescence spectrum shows a maximum fluorescence at 551 nm which is red-shifted by 24 nm from that recorded in solution. This red shift in the solid state is attributed to intermolecular interactions as in the solid state; the ground and excited state wave functions can be delocalized over many polymer chains. This results in a bathochromic shift of both the absorption and emission maxima with respect to the isolated species in solution. The PL quantum yields of **3a**−**e** were determined in DCM solution relative to a quinine sulfate standard. The values of PL quantum yield are higher than those of MEH-PPV (Φ_{PL} = 0.15). This may due to the *cis*,*trans* configuration and the branched side chain of these polymers which reduces interchain interactions. The solid-state absorption spectrum of **4e** shows a maximum absorption at 405 nm which is slightly red-shifted by 7 nm from that observed in solution. The solid-state fluorescence spectrum showed a maximum fluorescence at 526 nm which was red-shifted by 30 nm compared to the solution spectrum. Again, this red shift in solid state is attributed to intermolecular interactions. The PL quantum yields of polymers **4a**−**e** are almost identical, possibly due to all of these polymers having the same effective conjugation length and indicative of a weak dependence of PL quantum yield on polymer chain length. The values ($\Phi_{PL} \sim 0.47$) obtained are much higher than those for MEH−PPV (Φ_{PL} = 0.15) or **3c** (Φ_{PL} = 0.31). The reasons for this may due to *m*-phenylene linkages present in the polymer backbone that reduces interchain interactions.[46] However, the PL quantum efficiency obtained for **4a**−**e** are lower than that previously reported for poly(*m*-phenylene-vinylene-*alt*-2,5-dioctyloxy-*p*-phenylenevinylene)s ($\Phi_{PL} \sim$ 0.60). It appears that the regularly alternating *m*-phenylene linkages of this polymer lead to a higher quantum efficiency.[46]

The absorption and emission spectra of polymers **3f**−**h** and **4f**−**h** were recorded in dilute DCM solution (Figure 6). Polymer **3h** exhibited the longest conjugation length with an absorption maximum of 475 nm, which is red-shifted by 9 nm when compared to shortest conjugation length of **3f**. The fluorescence spectra recorded for **3f**−**h** shows nearly identical emission spectra for all of the chain lengths with the emission peak at 527 nm and a shoulder at 566 nm. The absorption maximum of the longest chain **3h** was slightly red-shifted by about 15 nm over that of an analogous polymer, poly(*p*-phenylenevinylene-*alt*-2,5-dioctyloxy-*p*-phenylenevinylene), reported previously. In addition, the emission maximum at 527 nm was also red-shifted by 10 nm when compared to that of polymers reported by Ferraris et al.[41] These observations can be rationalized by the random ROMP of **1** as discussed for the parent *cis*,*trans*-polymers. UV−vis spectra recorded for polymers **4f**−**h** exhibited two absorption bands. The two absorption bands for the longest polymer **4h** were observed at 319 and 402 nm, which were nearly identical when compared to the shortest length of polymer **4f**. The absorption spectra of **4f**−**h** were in agreement with previous reports for all *trans*-*m*,*p*-phenylenevinylene polymers.[43,44] The fluorescence spectra recorded for

4f−**h** shows nearly identical emission spectra for all chain lengths with the emission maximum peak at 495 nm and a shoulder at 526 nm. The wavelengths of these peaks are very similar to those observed for the *cis*,*trans*-vinylene polymers, **4a**, **4c**, and **4e**.

The electrochemical properties of polymers **3c** and **4c** were determined by cyclic voltammetry (CV) on thin films of the polymers deposited on a platinum working electrode held in an acetonitrile solution of $[(C_4H_9)_4N]PF_6$ (0.10 M) (Table 2). Films of **3c** with a *cis*,*trans*-microstructure exhibited a reversible oxidation at $E_{1/2}$ = 0.46 V against $Ag/AgNO_3$ and a reversible reduction at $E_{1/2}$ = −2.17 V with a color change in the film from orange (neutral) to dark blue (oxidized/reduced). The energy levels of the HOMO and LUMO are calculated to be −5.14 and −2.56 eV, respectively. These potentials were shifted to lower and higher values for polymers **3g** at $E_{1/2}$ = 0.43 V for oxidation and at $E_{1/2}$ = −2.15 V, respectively, after photoisomerization (HOMO = −5.11 eV and LUMO = −2.60 eV). This indicates that the *all-trans* polymer is easier to oxidize and reduce than the *cis*,*trans* polymer due to the more conjugated backbone structure. Films of **4c** with a *cis,trans* microstructure exhibited an irreversible oxidation at $E_{1/2}$ = 1.30 V against $Ag/AgNO_3$ and a reversible reduction at $E_{1/2}$ = −2.24 V (HOMO = −5.43 eV and LUMO = −2.48 eV). Films of **4g** with an *all-trans* microstructure exhibited an irreversible oxidation at $E_{1/2}$ = 1.00 V against $Ag/AgNO_3$ and a reversible reduction at $E_{1/2}$ = −2.41 V (HOMO = −5.40 eV and LUMO = −2.55 eV). The electrochemical band gap of the *all-trans* polymers (**3** and **4**) are lower than the *cis,trans* analogues. In the all *trans* structure the degree of conjugation is increased which causes a reduction in both the electrochemical and the optical band gap (see Table 3).

Thermogravimetric analysis of polymer **3** exhibited two major weight losses at around 300 °C (∼60% weight loss) and 500 °C (∼35% weight loss), and polymer **4** showed two major mass losses at around 400 °C (∼60% weight loss) and 550 °C (∼38% weight loss). These can be assigned to the loss of ethylhexyloxy side chains (theoretical weight 56%) and the volatilization of the polymer main chain (see Supporting Information). Investigation of the solid-state thermal behavior of **3e** by polarized optical microscopy showed little change when heated up to 250 °C and a color change to brown at 290 °C corresponding to decomposition of the polymer. No significant transitions were observed by DSC for polymer **3e** on either heating or cooling. A small transition in the DSC trace for polymer **4e** at −23 °C (ΔC_p = 0.2 J/(g °C)) is observed on heating and cooling. This second-order transition corresponds to the glass transition temperature (T_g) of **4e**. Crystallization of the side chains for **3** or **4** was not observed either on heating or cooling of these polymers.

Table 2. Optical Properties of Selected Polymers

	λ_{max}/nm		λ_{onset}/nm		λ_{PL}/nm		Φ_{PL}	E_{opt}/nm	
	solution	film	solution	film	solution	film	solution	solution	film
3a	462	477	523	556	527, 566	550	0.29	2.37	2.23
3c	464	477	523	557	527, 566	551	0.31	2.37	2.23
3e	467	479	524	561	527, 566	551	0.29	2.37	2.21
3f	466	480	530	563	527, 566	552	0.24	2.34	2.20
3g	468	480	530	563	527, 566	553	0.24	2.34	2.20
3h	475	481	532	565	527, 566	553	0.22	2.33	2.19
4a	313, 395	404	473	494	495, 525	526	0.44	2.62	2.51
4c	315, 397	404	479	494	495, 525	525	0.43	2.59	2.51
4e	315, 398	405	480	496	495, 525	526	0.47	2.58	2.50
4f	319, 402	409	486	504	495, 526	534	0.29	2.55	2.46
4g	319, 398	409	488	504	495, 526	534	0.29	2.54	2.46
4h	319, 402	410	486	504	495, 526	535	0.27	2.55	2.46

1,4-Phenylenevinylene and 1,3-Phenylenevinylene Block Copolymers. Block copolymers of poly(*p*-phenylenevinylene-2,5-diethylhexyloxy-*p*-phenylenevinylene), **3**, and poly(*m*-phenylenevinylene-2,5-diethylhexyloxy-*p*-phenylenevinylene), **4**, with different volume fractions were made by ROMP of **1** followed by addition of monomer **2**. In order to maximize the chances of forming desirable morphologies such as cylindrical and lamella, it was necessary to estimate the volume fractions and the length of the polymer. This was achieved by using estimates of the van der Waals volume of each monomer; the van der Waals volumes of repeat unit of **3** and **4** are both ∼300.98 cm^3/mol. Polymers were designed with volume fractions of 3:1 (**5a**), 1:1 (**5b**), and 1:3 (**5c**) by using the calculated repeat unit molar volumes. These volume fractions equate to degrees of polymerization of the constituent monomers of 15:5 (**5a**), 15:15 (**5b**), and 15:45 (**5c**). Scheme 2 shows the synthetic route employed to prepare block copolymers **5a**−**c**. Monomer **1** was dissolved in THF and ROMP was initiated by addition of a THF solution of the second generation Grubbs catalyst. The reaction mixture was heated at 40 °C and the conversion of monomer monitored by TLC. After complete consumption of monomer **1** a THF solution of monomer **2** was added to a polymerization reaction at the same temperature. The reaction was finally quenched by addition of an excess of ethyl vinyl ether at room temperature. The resulting block copolymers were purified by filtering through a short plug of silica gel and isolated by evaporation of the solvent.

For block copolymer **5a**, a M_n of 13 200 (expected M_n = 9304) with a polydispersity of 1.76 was observed, a M_n of 17 600 (expected M_n = 13 904) with a polydispersity of 1.67 was obtained for **5b**, and a M_n of 32 800 (expected M_n = 27 704) with a polydispersity of 1.46 was obtained for **5c** (Supporting Information). The polydispersities of the block copolymers are comparable to or higher than the polydispersity (1.46) of the starting homopolymer **3b**. This is presumably due to intramolecular chain transfer reactions that

Table 3. Electrochemical Properties of Selected Polymers

	oxidation[a]		reduction[a]				
sample	$E_{1/2}$/vs $Ag/AgNO_3$	onset	$E_{1/2}$/vs $Ag/AgNO_3$	onset	HOMO/eV[b]	LUMO/eV[c]	E_{ec}/eV[d]
3c	0.464	0.441	−2.171	−2.136	−5.14	−2.56	2.58
3g	0.432	0.420	−2.154	−2.094	−5.11	−2.60	2.51
4c	1.297 (ir)	0.736	−2.243	−2.214	−5.43	−2.48	2.95
4g	1.001 (ir)	0.705	−2.406	−2.150	−5.40	−2.55	2.85
5a	1.116 (ir)	0.524	−2.318	−2.167	−5.22	−2.53	2.69
5d	0.593	0.471	−2.200	−2.080	−5.17	−2.62	2.55
5b	1.284 (ir)	0.624	−2.507	−2.236	−5.32	−2.46	2.86
5c	0.979 (ir)	0.696	−2.446	−2.185	−5.39	−2.51	2.88

[a] CV of polymer films on Pt plate were measured in MeCN solution containing 0.10 M n-Bu_4NPF_6. [b] HOMO = $-(4.8 + E_{pa\text{-}onset} - E_{Fc})$. Half-wave potential of ferrocene, E_{Fc} (= 0.105 V vs $Ag/AgNO_3$), was measured in MeCN solution. [c] LUMO = $-(4.8 + E_{pc\text{-}onset} - E_{Fc})$. [d] Electrochemical band gap was calculated from E_{ec} = LUMO − HOMO.

Scheme 2. Synthetic Route to Block Copolymers 5 (R = 2-Ethylhexyl)

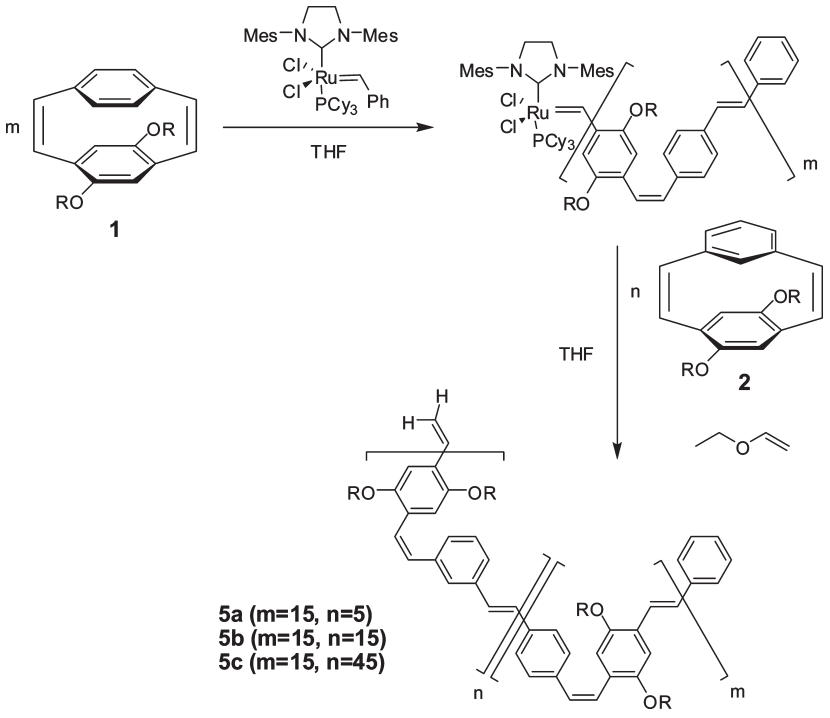

take place during the extended reaction time needed to prepare the block copolymers. The polydispersity decreases with increasing chain length as expected. The ^{1}H NMR spectra of the block copolymers **5a**−**c** (Figure 7) confirmed the incorporation of blocks derived from monomers **1** and **2** and that the backbone is made up of *cis*- and *trans*-vinylene linkages. Peaks at 3.95 and 3.47 ppm can be assigned to the hydrogens of the methylene groups attached to the oxygen for the *trans*- and *cis*-vinylene links of the backbone of polymer **3**, respectively. Peaks at 3.95 and 3.42 ppm were associated with the methylene groups attached to the oxygen for the *trans*- and *cis*-vinylene linkages of polymer **4**. Integration of these signals was difficult as the chemical shifts of these signals overlap. However, it is clear from the spectra of the copolymers **5a**−**c** that as the volume fraction of blocks derived from **2** increased, the intensity of the signal at 3.42 ppm increased, as expected. A peak at 4.00 ppm was observed in the ^{1}H NMR spectrum of polymers **5a**−**c**. Observation of this signal suggests that a small amount of the *all-trans*-form of the polymer was present in these polymers, presumably due to the extended reaction time.

Absolute values for the degree of polymerization in **5a**−**c** were determined using the ^{1}H NMR spectrum by integration of the signals for the vinyl end groups observed at around 5.23 and 5.75 ppm against those for the methylene groups attached to oxygen. Again, the values obtained are higher than expected for the catalyst:monomer ratio employed. This suggests that secondary metathesis reactions may occur during the polymerization. The end groups of the polymer were also be analyzed by MALDI-TOF mass spectrometry. The results of MALDI-TOF mass spectrometry depend strongly on the sample and the matrix preparation, and it was difficult to obtain high-quality spectra for the higher molecular weight polymers **5b** and **5c**.[47,48]

The MALDI-TOF mass spectrum of **5a** (Figure 8) shows a main series of peaks separated by an interval of 460 mass units, corresponding to the molecular weight of monomers **1** and **2**. This series (▲) is consistent with **5a** capped with vinyl and phenyl end groups. A further series of peaks are also observed: the series (●) at 102 mass units (C_8H_6) less than the major series can be attributed to the formation of linear polymers with one less phenylenevinylene unit, and the series of peaks (○) at 358 less than the primary series can be assigned to to those polymers with one less diethylhexyloxy-substituted phenylenevinylene unit. These sequences are consistent with intramolecular secondary metathesis before termination. Low molar mass cyclic oligomers (■) generated by this reaction are observed with one extra diethylhexyloxy-substituted phenylenevinylene unit ($C_{24}H_{38}O_2$, mass = 358). Again, there is no evidence for intermolecular chain transfer reactions as no peaks are detected for polymers with two phenyl or two vinyl end groups.

Polymers **5a** can be isomerized to the *trans*-vinylene polymers **5d** by prolonged irradiation at 365 nm in THF solution (10 mg in 10 mL). The isomerization was followed by ^{1}H NMR spectroscopy (see Supporting Information), and 95% complete conversion was achieved by irradiation for 36 h. The disappearance of the signals between 6.60 and 6.90 ppm associated with the *cis*-vinylene unit and the phenyl groups neighboring to *cis*-vinylene groups confirmed the isomerization to an *all-trans*-vinylene configuration.

The UV−vis absorption spectra of block copolymers **5a**−**c** were recorded in dilute DCM solution (Figure 9). The observation of three bands at 315, 400, and 468 nm is consistent with the presence of blocks derived from monomer **1** (e.g., **3b** λ_{max} = 463 nm) and monomer **2** (**4b**, λ_{max} = 317 and 398 nm). Copolymer **5a** has a higher content of polymer **3**; therefore, the profile of the absorption spectrum of **5a** is dominated by that of polymer **3**, and an absorption maximum is observed at 468 nm. Polymer **5b** has equal volume fractions of polymers **3** and **4**, and the absorption spectrum reflects this distribution of chain lengths. Block copolymer **5c** has the largest percentage of polymer **4** by volume and molar ratio, and therefore the absorption spectrum is dominated by the absorption of polymer **4**. The absorption spectra of the block copolymers **5a**−**c** can be interpreted as the weighted average of the chromophores of the constituent homopolymers **3** and **4**.

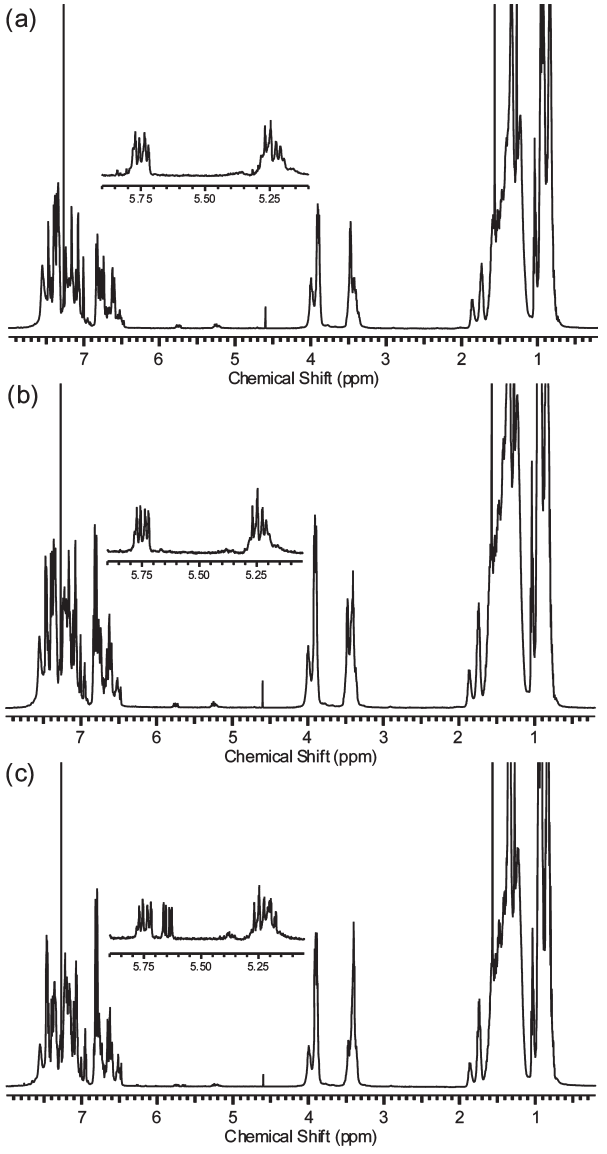

Figure 7. ^{1}H NMR spectra of (a) **5a**, (b) **5b**, and (c) **5c** in $CDCl_3$ solution.

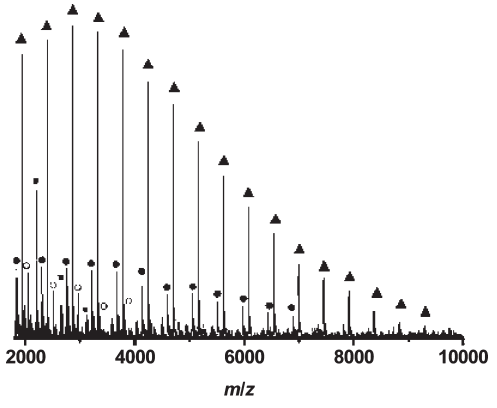

Figure 8. MALDI-TOF mass spectrum of block copolymer **5a**.

The photoluminescence of copolymers **5a**−**c** were examined in dilute DCM solution. When solutions were excited at 465 nm, the emission spectra (Figure 10a) are nearly identical for **5a**−**c** with an emission maximum at 527 nm and a shoulder at 569 nm. This emission is consistent with that of

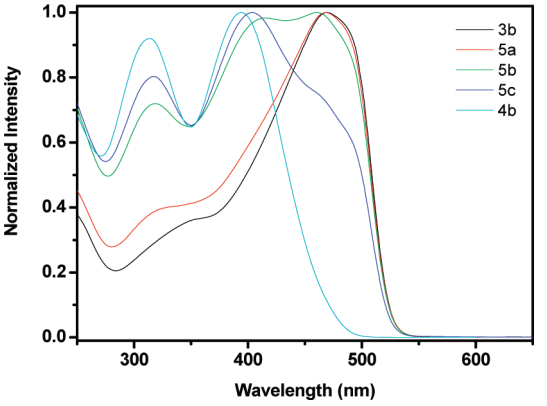

Figure 9. Solution UV−vis spectra of **3b, 4b**, and **5a**−**c**.

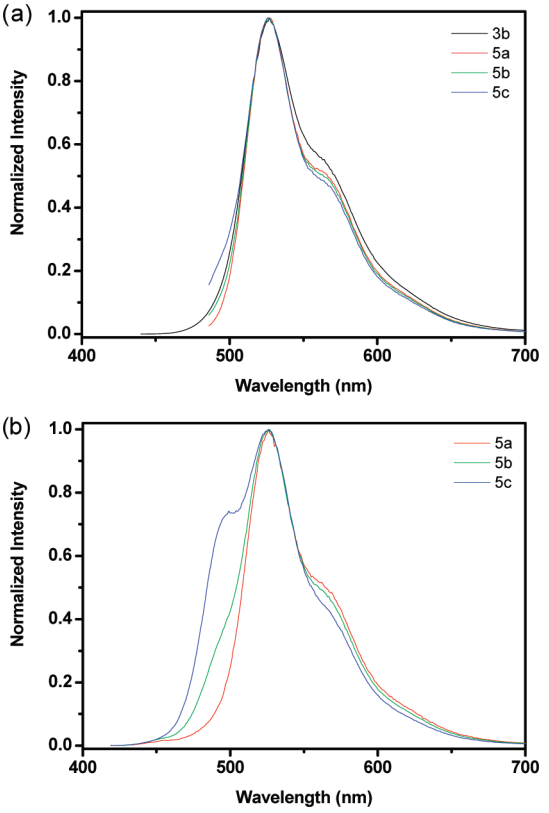

Figure 10. Solution PL spectra of **5a**−**c**: (a) excitation at 465 nm; (b) excitation at 390 nm.

polymer **3** (e.g., **3a**−**e**, λ_{max} = 527 nm), and this observation was expected as the excitation wavelength is close to the absorption maximum of polymer **3** (**3a**, λ_{max} = 462 nm) and is in a region where polymer **4** does not absorb strongly. However, when polymer solutions were excited at 390 nm, close to the maximum absorption of polymer **4** and in a region where polymer **3** is less absorbing, the emission maximum is dominated by a peak at 527 nm for polymer **3**. This indicates that energy transfer from the block with the larger optical band gap (**4**) to that with the smaller band gap (**3**) is almost complete. A shoulder at 495 nm (Figure 10b) on the main emission peak can be seen for copolymers **5b** and **5c**. The relative intensity of this peak increases with the mole fraction of the higher band gap polymer **4**. This suggests that the energy transfer was not complete in block copolymers with very long chains of the higher band gap polymer. Solid-state photoluminescence of copolymers **5a**−**c** was examined

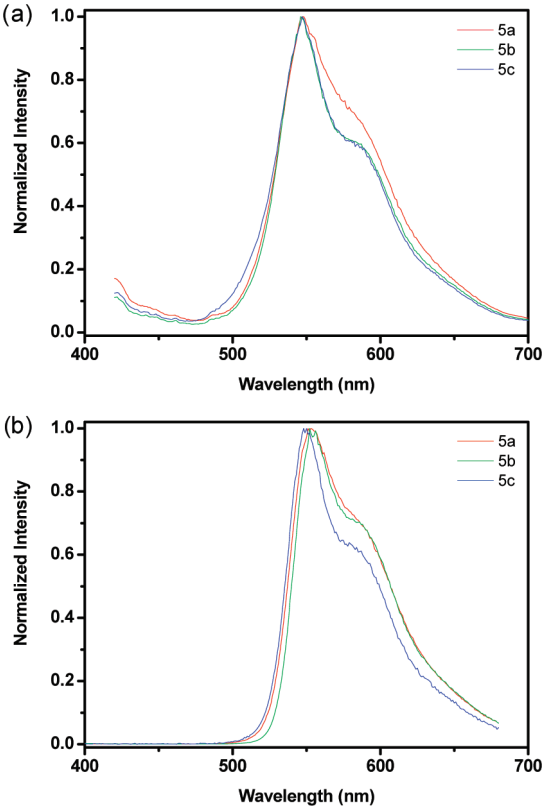

Figure 11. Solid-state PL spectra of **5a**−**c**: (a) excitation at 465 nm; (b) excitation at 370 nm.

by spin-casting thin films from a chloroform solution onto a Spectrasil substrate. When the films were excited at 465 nm, the fluorescence spectra of **5a**−**c** are very similar, with an emission maximum at 547 nm and a shoulder at around 589 nm. These spectra are very similar to the solid-state spectra of homopolymers **3a**−**e**. It appears that emission occurs from the most conjugated segment of the polymer, regardless of the chain length (Figure 11a) and energy transfer is efficient. Excitation at 370 nm gave an emission maximum at 547 nm with a shoulder at 589 nm (Figure 11b). This is again consistent with that of homopolymers **3a**−**e**; importantly, no emission was observed at 495 nm, and this suggests that energy transfer is more effective in the solid state for copolymers **5a**−**c**. The PL quantum yields ($\Phi_{PL} \sim 0.30$) of block copolymers **5a**−**c** are very similar and independent of the composition.

The energy of the band gap in the solid-state ($E_g = 2.69$ eV for **5a**; $E_g = 2.86$ eV for **5b**; $E_g = 2.88$ eV for **5c**) increases as the content of polymer **4** increases. Following the results obtained for the HOMO level in the solid state ($E_{HOMO} = -5.22$ eV for **5a**; $E_{HOMO} = -5.32$ eV for **5b**; $E_{HOMO} = -5.39$ eV for **5c**). However, the values of the LUMO level ($E_{LUMO} = -2.53$ eV for **5a**; $E_{LUMO} = -2.46$ eV for **5b**; $E_{LUMO} = 2.51$ eV for **5c**) are all the same within experimental error. The energy of the band gap in the solid state decreases after photoisomerization of *cis,trans*-**5a** ($E_g = 2.69$ eV) to *all-trans*-**5d** ($E_g = 2.55$ eV). The increase in conjugation length for the *all-trans* structure leads to a reduction in the electrochemical band gap.

Thermogravimetric analysis of the block copolymers **5a**−**c** showed two main mass losses, presumably due to the decomposition of the side chains and then the polymer main chain (Supporting Information). The first decomposition was found at 403 °C for **5a**, 404 °C for **5b**, and 407 °C for **5c**. The second decomposition occurs at 647 °C for **5a**, 651 °C for **5b**, and 655 °C for **5c**. These results suggest that polymers **5a**−**c** show comparable thermal stability. Polarized optical microscopy of **5a**−**c** showed little change on heating to 400 °C, at which point the color changed to brown, indicative of decomposition of the polymer. The DSC traces of **5a**−**c** showed a small transition at around −5 °C (see Supporting Information). This transition was attributed to the glass transition temperature of polymer **4**; no transitions for the polymer **3** were observed. The presence of a glass transition for bulk **4** in the DSC of the block copolymers **5a**−**c** suggests that phase separation of the two blocks is occurring in the solid state. However, initial studies of the solid-state morphology by AFM and X-ray diffraction have been inconclusive due to the limited contrast between the blocks of **5a**−**c**.

Conclusions

Ring-opening metathesis polymerization of strained cyclophanedienes using ruthenium carbene complexes (Grubbs 2 catalyst) gives phenylenevinylene homopolymers and block copolymers with control of the polymer molecular weight and block volume fraction. Metathesis of only one vinylene group of the cyclophanediene leads to polymers with a backbone of alternating *cis*- and *trans*-vinylene linkages with little or no control of the regiochemistry of the ring-opening for asymmetric cyclophanediene monomers. The as-formed polymers can be photochemically isomerized to the *all-trans*-vinylene derivatives with a decrease in the electrochemical band gap of the polymers consistent with an increase in the conjugation length. The solid-state UV−vis absorption and fluorescence spectra of the block copolymers indicate that there is efficient energy transfer between the different blocks of the copolymers.

Experimental Section

Chemicals. Unless otherwise noted, all reagents were used as received from Lancaster and Aldrich without further purification. THF was distilled under a nitrogen atmosphere over sodium/benzophenone ketyl.

Synthesis. Monomers, diethylhexyloxy-substituted paracyclophanediene DEHOPCPDE (**1**), and diethylhexyloxy-substituted metaparacyclophanediene DEHOMPCPDE (**2**) were prepared by a modification of established procedures.[32,33] The homopolymers and block copolymers are prepared as described below.

Synthesis of Poly(*p*-phenylenevinylene-2,5-diethylhexyloxy-*p*-phenylenevinylene)s (3). In a nitrogen-filled Radleys GreenHouse, **1** (46 mg, 0.1 mmol) was charged into five separate tubes and dissolved in 1.6, 1.2, 0.8, 0.64, and 0.53 mL of dry THF. The second generation Grubbs catalyst (33 mg) was dissolved in 3.3 mL of dry THF and stirred for at least 10 min. Aliquots of the catalyst solution (849, 569, 425, 340, and 280 μL) were then added into the monomer solutions prepared previously and the GreenHouse heated at 40 °C for 20 h. The reaction mixtures were cooled to room temperature, and excess ethyl vinyl ether (2 mL) was added to quench the reaction. After stirring for a further 4 h at room temperature, the reaction mixtures were concentrated in vacuo. The products were redissolved in chloroform and filtered through a short plug of silica to remove the catalyst. The solvent was removed under reduced pressure, and the resulting polymers were obtained in the range of 83%−95% yield. Polymer **3a** (yield: 95%). ^{1}H NMR (500 MHz, $CDCl_3$): δ 6.45−7.70 (br m, 10H), 5.69−5.83 (br d, 0.09H), 5.16−5.34 (br d, 0.09H), 3.85−4.15 (br m, 2H), 3.41−3.65 (br m, 2H), 1.11−1.90 (br m, 18H), 0.76−1.05 ppm (br t, 12H). MALDI-TOF MS for polymer **3a**: repeat unit = 460 g/mol. Calculated for **3a** ($C_{328}H_{448}O_{20}$): C, 83.62; H, 9.59. Found: C, 81.97; H,

8.46. Polymer **3b** (yield: 86%). ^{1}H NMR (500 MHz, $CDCl_3$): δ 6.45−7.70 (br m, 10H), 5.71−5.84 (br d, 0.07H), 5.15−5.33 (br d, 0.07H), 3.85−4.14 (br m, 2H), 3.41−3.68 (br m, 2H), 1.11−1.90 (br m, 18H), 0.76−1.05 ppm (br t, 12H). MALDI-TOF MS for polymer **3b**: repeat unit = 460 g/mol. Calculated for **3b** ($C_{488}H_{668}O_{30}$): C, 83.56; H, 9.60. Found: C, 81.63; H, 8.12. Polymer **3c** (yield: 83%). ^{1}H NMR (500 MHz, $CDCl_3$): δ 6.45−7.70 (br m, 10H), 5.69−5.84 (br d, 0.05H), 5.16−5.34 (br d, 0.05H), 3.85−4.15 (br m, 2H), 3.42−3.66 (br m, 2H), 1.11−1.90 (br m, 18H), 0.76−1.05 ppm (br t, 12H). Polymer **3d** (yield: 91%). ^{1}H NMR (500 MHz, $CDCl_3$): δ 6.45−7.70 (br m, 10H), 5.70−5.84 (br d, 0.04H), 5.16−5.35 (br d, 0.04H), 3.85−4.18 (br m, 2H), 3.41−3.68 (br m, 2H), 1.11−1.90 (br m, 18H), 0.76−1.05 ppm (br t, 12H). Polymer **3e** (yield: 92%). ^{1}H NMR (500 MHz, $CDCl_3$): δ 6.45−7.70 (br m, 10H), 5.70−5.85 (br d, 0.03H), 5.15−5.34 (br d, 0.03H), 3.85−4.17 (br m, 2H), 3.40−3.67 (br m, 2H), 1.11−1.90 (br m, 18H), 0.76−1.05 ppm (br t, 12H).

Synthesis of Poly(*m*-phenylenevinylene-2,5-diethylhexyloxy-*p*-phenylenevinylene)s (4). As for poly(*p*-phenylenevinylene-2,5-diethylhexyloxy-*p*-phenylenevinylene)s above using the same amount of monomer **2** and catalyst. The resulting polymers were obtained in the range of 89%−97% yield. Polymer **4a** (yield: 92%). ^{1}H NMR (500 MHz, $CDCl_3$): δ 6.45−7.70 (br m, 10H), 5.71−5.82 (br d, 0.09H), 5.16−5.33 (br d, 0.09H), 3.83−4.07 (br m, 2H), 3.32−3.55 (br m, 2H), 1.11−1.91 (br m, 18H), 0.76−1.06 ppm (br t, 12H). MALDI-TOF MS for polymer **4a**: repeat unit = 460 g/mol. Calculated for **4a** ($C_{328}H_{448}O_{20}$): C, 83.62; H, 9.59. Found: C, 81.92; H, 8.87. Polymer **4b** (yield: 97%). ^{1}H NMR (500 MHz, $CDCl_3$): δ 6.45−7.70 (br m, 10H), 5.71−5.81 (br d, 0.07H), 5.16−5.34 (br d, 0.07H), 3.85−4.09 (br m, 2H), 3.32−3.55 (br m, 2H), 1.12−1.91 (br m, 18H), 0.75−1.05 ppm (br t, 12H). MALDI-TOF MS for polymer **4b**: repeat unit = 460 g/mol. Calculated for **4b** ($C_{488}H_{668}O_{30}$): C, 83.56; H, 9.60. Found: C, 81.70; H, 8.66. Polymer **4c** (yield: 93%). ^{1}H NMR (500 MHz, $CDCl_3$): δ 6.45−7.70 (br m, 10H), 5.70−5.81 (br d, 0.05H), 5.16−5.33 (br d, 0.05H), 3.84−4.10 (br m, 2H), 3.32−3.56 (br m, 2H), 1.12−1.91 (br m, 18H), 0.76−1.06 ppm (br t, 12H). Polymer **4d** (yield: 91%). ^{1}H NMR (500 MHz, $CDCl_3$): δ 6.45−7.70 (br m, 10H), 5.71−5.81 (br d, 0.04H), 5.15−5.33 (br d, 0.04H), 3.85−4.10 (br m, 2H), 3.32−3.57 (br m, 2H), 1.11−1.92 (br m, 18H), 0.76−1.06 ppm (br t, 12H). Polymer **4e** (yield: 89%). ^{1}H NMR (500 MHz, $CDCl_3$): δ 6.45−7.70 (br m, 10H), 5.69−5.82 (br d, 0.03H), 5.15−5.35 (br d, 0.03H), 3.83−4.11 (br m, 2H), 3.32−3.57 (br m, 2H), 1.11−1.94 (br m, 18H), 0.76−1.08 ppm (br t, 12H).

Synthesis of Poly(*p*-phenylenevinylene-2,5-diethylhexyloxy-*p*-phenylenevinylene-*b*-*m*-phenylenevinylene-2,5-diethylhexyloxy-*p*-phenylenevinylene)s (5). In a nitrogen-filled Radleys GreenHouse, **1** (48.3 mg, 0.105 mmol) was charged into three separate tubes and dissolved in 1.2 mL of dry THF individually. Second generation Grubbs catalyst (22 mg) was dissolved in 2.2 mL of dry THF and stirred for at least 10 min. Aliquots of the catalyst solution (594 μL) were then added into the monomer solutions prepared previously and the GreenHouse heated at 40 °C for 20 h. Compound **2** (209.3 mg) was dissolved in 3.9 mL of dry THF. Aliquots of the **2** solution (300 μL, 900 μL, 2.7 mL) were then added into the reaction mixtures and the GreenHouse heated at 40 °C for another 24 h. The reaction mixtures were cooled to room temperature, and excess ethyl vinyl ether (2 mL) was added to quench the reaction. After stirring for a further 4 h at room temperature, the reaction mixtures were concentrated in vacuo. The products were redissolved in chloroform and filtered through a short plug of silica to remove the catalyst. The solvent was removed under reduced pressure, and the resulting copolymers were obtained in the range of 88%−94% yield. Copolymer **5a** (yield: 88%). ^{1}H NMR (500 MHz, $CDCl_3$): δ 7.28−7.64 (br m, 5H), 6.97−7.26 (br m, 3H), 6.46−6.86 (br m, 3H), 5.70−5.80 (br d, 0.05H), 5.18−5.32 (br d, 0.06H), 3.85−4.05 (br m, 2H), 3.32−3.54 (br m, 2H), 1.10−1.90 (br m, 18H), 0.75−1.06 ppm (br m, 12H). MALDI-TOF MS for polymer **5a**: repeat unit = 460 g/mol. Calculated for **5a** ($C_{648}H_{888}O_{40}$): C, 83.53; H, 9.61. Found: C, 82.35; H, 9.40. Copolymer **5b** (yield: 94%). ^{1}H NMR (500 MHz, $CDCl_3$): δ 7.28−7.63 (br m, 4H), 6.93−7.26 (br m, 3.5H), 6.47−6.86 (br m, 3H), 5.70−5.80 (br d, 0.03H), 5.17−5.30 (br d, 0.03H), 3.84−4.06 (br m, 2H), 3.32−3.54 (br m, 2H), 1.10−1.92 (br m, 18H), 0.75−1.06 ppm (br m, 12H). Calculated for **5b** ($C_{968}H_{1328}O_{60}$): C, 83.49; H, 9.61. Found: C, 82.72; H, 9.66. Copolymer **5c** (yield: 90%). ^{1}H NMR (500 MHz, $CDCl_3$): δ 7.28−7.60 (br m, 3.4H), 6.93−7.26 (br m, 4H), 6.47−6.81 (br m, 3H), 5.62−5.78 (br d, 0.02H), 5.16−5.31 (br d, 0.02H), 3.83−4.07 (br m, 2H), 3.32−3.53 (br m, 2H), 1.12−1.91 (br m, 18H), 0.74−1.06 ppm (br m, 12H). Calculated for **5c** ($C_{1928}H_{2648}O_{120}$): C, 83.46; H, 9.62. Found: C, 82.35; H, 9.47.

Measurements. ^{1}H NMR spectra were recorded in deuterated chloroform or deuterated dichloromethane with chemical shifts using residual deuterated solvent as an internal standard on a Bruker Ultrashield 500 MHz or a Varian Inova 300 MHz spectrometer. Elemental analyses were determined using a Carlo Erba Instruments EA1108 Elemental Analyzer. MALDI-TOF mass spectra were obtained on a Micromass TOF Spec 2E instrument using dithranol as the matrix. Gel permeation chromatography was carried out in THF using a Viscotek GPCmax VE2001 solvent/sample module with 2 × PL gel 10 μm MIXED-B + 1 × PL gel 500A columns, a Viscotek VE3580 RI detector, and a VE 3240 UV/vis multichannel detector. The flow rate was 1 mL/min, and the system was calibrated with low-polydispersity polystyrene standards in the range of 200 to 180 × 10^4 g/mol from Polymer Laboratories. The analyzed samples contained *n*-dodecane as a flow marker. UV−vis measurements were obtained on a Varian Cary 5000 UV−vis−NIR spectrophotometer. Photoluminescence measurements were carried out on a Varian Cary Eclipse fluorescence spectrophotometer. Films were spin-coated from chloroform or benzene at 1000 rpm for 90 s. The solution quantum yields were measured in dilute DCM solution. The absorbance of the sample solution was kept below 0.05 to avoid inner filter effect. Measurements were performed at room temperature, while both sample and quinine sulfate solutions were excited at the same wavelength (370 nm) to avoid possible error caused by neglecting the difference between the excitation light intensities of different wavelengths. Cyclic voltammetry (CV) was performed at 100 mV s^{-1} in a BASI Epsilon electrochemical workstation with a three-electrode cell, $Ag/AgNO_3$ as reference electrode, platinum wire as counter electrode, and polymer film on a platinum plate as the working electrode in nitrogen-purged anhydrous 0.1 M tetrabutylammonium hexafluorophosphate−acetonitrile solution at room temperature. Thermal properties were studied by thermogravimetric analysis on a TA TGA Q5000 (scan rate 20 °C/min), differential scanning calorimetry using a Perkin-Elmer Diamond (scan rate 20 °C/min), and polarized optical microscopy on an Olympus BH2 microscope attached to a temperature controller module Linkam TMS 94 hot stage. The photoisomerization was carried out using SYNGENE GLLS-6 UV lamp (LF-206LS 6W tube) at 365 nm. The polymer was placed in shield box and irradiated at a distance of 10 cm to obtain an *all-trans*-structure.

Acknowledgment. Financial support from the UK DTI, the EPSRC, and the University of Manchester is gratefully acknowledged.

Supporting Information Available: Spectroscopic and analytical data of polymers, GPC curves, and NMR spectra. This material is available free of charge via the Internet at http://pubs.acs.org.

References and Notes

(1) Kugler, T.; Logdlund, M.; Salaneck, W. R. *Acc. Chem. Res.* **1999**, *32*, 225–234.

(2) Friend, R. H.; Gymer, R. W.; Holmes, A. B.; Burroughes, J. H.; Marks, R. N.; Taliani, C.; Bradley, D. D. C.; Dos Santos, D. A.; Bredas, J. L.; Logdlund, M.; Salaneck, W. R. *Nature* **1999**, *397*, 121–128.
(3) Zaumseil, J.; Sirringhaus, H. *Chem. Rev.* **2007**, *107*, 1296–1323.
(4) Naber, R. C. G.; Tanase, C.; Blom, P. W. M.; Gelinck, G. H.; Marsman, A. W.; Touwslager, F. J.; Setayesh, S.; De Leeuw, D. M. *Nat. Mater.* **2005**, *4*, 243–248.
(5) Gunes, S.; Neugebauer, H.; Sariciftci, N. S. *Chem. Rev.* **2007**, *107*, 1324–1338.
(6) Schmidt-Mende, L.; Fechtenkotter, A.; Mullen, K.; Moons, E.; Friend, R. H.; MacKenzie, J. D. *Science* **2001**, *293*, 1119–1122.
(7) Burroughes, J. H.; Bradley, D. D. C.; Brown, A. R.; Marks, R. N.; Mackay, K.; Friend, R. H.; Burns, P. L.; Holmes, A. B. *Nature* **1990**, *347*, 539–541.
(8) Wessling, R. A. *J. Polym. Sci., Polym. Symp.* **1985**, *72*, 55–66.
(9) Gilch, H. G.; Wheelwright, W. L. *J. Polym. Sci., Part A: Polym. Chem.* **1966**, *4*, 1337.
(10) Rost, H.; Teuschel, A.; Pfeiffer, S.; Horhold, H. H. *Synth. Met.* **1997**, *84*, 269–270.
(11) Bao, Z. N.; Chen, Y. M.; Cai, R. B.; Yu, L. P. *Macromolecules* **1993**, *26*, 5281–5286.
(12) Yu, L. P.; Bao, Z. N. *Adv. Mater.* **1994**, *6*, 156–159.
(13) Miao, Y. J.; Bazan, G. C. *J. Am. Chem. Soc.* **1994**, *116*, 9379–9380.
(14) Edwards, J. H.; Feast, W. J. *Polymer* **1980**, *21*, 595–596.
(15) Gorman, C. B.; Ginsburg, E. J.; Sailor, M. J.; Moore, J. S.; Jozefiak, T. H.; Lewis, N. S.; Grubbs, R. H.; Marder, S. R.; Perry, J. W. *Synth. Met.* **1991**, *41*, 1033–1038.
(16) Jozefiak, T. H.; Ginsburg, E. J.; Gorman, C. B.; Grubbs, R. H.; Lewis, N. S. *J. Am. Chem. Soc.* **1993**, *115*, 4705–4713.
(17) Thorn-Csányi, E.; Hohnk, H. D.; Pflug, K. P. *J. Mol. Catal.* **1993**, *84*, 253–259.
(18) Thorn-Csányi, E.; Pleug, K. P. *Macromol. Chem.* **1993**, *194*, 2287–2294.
(19) Thorn-Csányi, E.; Kraxner, P.; Hammer, J. *J. Mol. Catal.* **1994**, *90*, 15–20.
(20) Conticello, V. P.; Gin, D. L.; Grubbs, R. H. *J. Am. Chem. Soc.* **1992**, *114*, 9708–9710.
(21) Miao, Y. J.; Bazan, G. C. *Macromolecules* **1994**, *27*, 1063–1064.
(22) Yu, C.-Y.; Turner, M. L. *Angew. Chem., Int. Ed.* **2006**, *45*, 7797–7800.
(23) Yu, C.-Y.; Kingsley, J. W.; Lidzey, D. G.; Turner, M. L. *Macromol. Rapid Commun.*, DOI: 10.1002/marc.200900345.
(24) Matsen, M. W.; Bates, F. S. *Macromolecules* **1996**, *29*, 1091–1098.
(25) Matsen, M. W.; Thompson, R. B. *J. Chem. Phys.* **1999**, *111*, 7139–7146.
(26) Klok, H. A.; Lecommandoux, S. *Adv. Mater.* **2001**, *13*, 1217–1229.
(27) Krevelen, D. W. V. *Properties of Polymers - Their Correlation with Chemical Structure; Their Numerical Estimation and Prediction from Additive Group Contributions*; Elsevier: Amsterdam, 1990.
(28) Asawapirom, U.; Guntner, R.; Forster, M.; Scherf, U. *Thin Solid Films* **2005**, *477*, 48–52.
(29) Schmitt, C.; Nothofer, H. G.; Falcou, A.; Scherf, U. *Macromol. Rapid Commun.* **2001**, *22*, 624–628.
(30) Scherf, U.; List, E. J. W. *Adv. Mater.* **2002**, *14*, 477.
(31) Tu, G. L.; Li, H. B.; Forster, M.; Heiderhoff, R.; Balk, L. J.; Scherf, U. *Macromolecules* **2006**, *39*, 4327–4331.
(32) Scherf, U.; Gutacker, A.; Koenen, N. *Acc. Chem. Res.* **2008**, *41*, 1086–1097.
(33) Wang, H. B.; Ng, M. K.; Wang, L. M.; Yu, L. P.; Lin, B. H.; Meron, M.; Xiao, Y. N. *Chem. Eur. J.* **2002**, *8*, 3246–3253.
(34) Liang, Y. Y.; Wang, H. B.; Yuan, S. W.; Lee, Y. G.; Yu, L. P. *J. Mater. Chem.* **2007**, *17*, 2183–2194.
(35) Mitchell, R. H.; Otsubo, T.; Boekelheide, V. *Tetrahedron Lett.* **1975**, *16*, 219–222.
(36) Potter, S. E.; Sutherland, I. O. *J. Chem. Soc., Chem. Commun.* **1973**, *15*, 520–521.
(37) Wagaman, M. W.; Grubbs, R. H. *Macromolecules* **1997**, *30*, 3978–3985.
(38) Thorn-Csányi, E.; Kraxner, P.; Strachota, A. *Macromol. Rapid Commun.* **1998**, *19*, 223–228.
(39) Liao, L.; Pang, Y.; Ding, L. M.; Karasz, F. E. *Macromolecules* **2001**, *34*, 6756–6760.
(40) Haigh, D. M.; Kenwright, A. M.; Khosravi, E. *Tetrahedron* **2004**, *60*, 7217–7224.
(41) Barashkov, N. N.; Guerrero, D. J.; Olivos, H. J.; Ferraris, J. P. *Synth. Met.* **1995**, *75*, 153–160.
(42) Hu, B.; Karasz, F. E. *Synth. Met.* **1998**, *92*, 157–160.
(43) Li, J. A.; Pang, Y. *Synth. Met.* **2004**, *140*, 43–48.
(44) Drury, A.; Maier, S.; Ruther, M.; Blau, W. J. *J. Mater. Chem.* **2003**, *13*, 485–490.
(45) Dufresne, G.; Bouchard, J.; Belletete, M.; Durocher, G.; Leclerc, M. *Macromolecules* **2000**, *33*, 8252–8257.
(46) Pang, Y.; Li, J.; Hu, B.; Karasz, F. E. *Macromolecules* **1999**, *32*, 3946–3950.
(47) Anders, U.; Nuyken, O.; Buchmeiser, M. R.; Wurst, K. *Macromolecules* **2002**, *35*, 9029–9038.
(48) Klarner, G.; Former, C.; Martin, K.; Rader, J.; Mullen, K. *Macromolecules* **1998**, *31*, 3571–3577.